Article

Hydrophobic Interface Cages in Microemulsions: Concept and Experiment Using Tetraphenylethylene-based Double-tailed Surfactant

GUAN Weijiang, TANG Xiaofang, WANG Wei, LIN Yanjun and LU Chao✉

Received September 25, 2020
Accepted November 19, 2020

Although hydrophobic interface regions adjacent to water droplets play a vital role in microemulsion-based studies, their widespread applications have not been explicitly evoked owing to their small spaces. Herein, we designed and synthesized a novel double-tailed anionic surfactant(TPE-di-C8SS) by linking the propeller-shaped tetraphenylethylene(TPE) with two octyl chains and an anionic sulfonate headgroup through a methoxybutyl spacer. The extra spacer and steric hindrance between rigid TPE groups can create the large cavities in hydrophobic interface regions, which we call the hydrophobic interface cages(HICs). The potentials and advantages of HICs in the easily-prepared TPE-di-C8SS microemulsion have been implemented by comparing the extraction efficiency towards cationic rhodamine B with Aerosol OT(AOT) microemulsion. The results provided solid evidence that HICs rather than water droplets contributed to a higher extraction efficiency. This work not only proposes a concept of HICs but also provides a new perspective of their utilization in microemulsion-based applications.

Keywords Aggregation-induced emission; Hydrophobic interface cage; Tetraphenylethylene; Microemulsion

1 Introduction

Water-in-oil(w/o) microemulsions have been extensively applied for biphasic reactions[1,2], liquid extractions[3,4], biomolecule stabilizations[5,6], soft-template nanomaterial syntheses[7,8], and so on. Undoubtedly, these great successes are attributed to the versatile Aerosol OT(AOT) surfactant and nanometer-sized water droplets[1—10]. AOT could stabilize water droplets in oils without the aid of cosurfactants, while water droplets are responsible for solubilizing polar and ionic substances in oils[9,10]. More interestingly, some researchers pioneered that it is not only water droplets but also hydrophobic interface regions adjacent to water droplets play a vital role in microemulsion-based applications[11—18]. For example, the negatively charged 8-hydroxypyrene-1,3,6-trisulfonate, which was electrostatically attracted to the water-oil interface of cetyltrimethylammonium bromide microemulsion, was partially resided in hydrophobic interface regions[17]. Moreover, $[VO_2dipic]^-$, a well-known metal complex with high charge and polarity, was embedded in hydrophobic interface regions of AOT microemulsion rather than water droplets[18]. These pioneering findings revealed that hydrophobic interface regions can serve as the indispensable complementary to water droplets in microemulsion-based studies. However, the application potentials of hydrophobic interface regions have hardly been explored owing to the small cavities in the current hydrophobic interface regions. Therefore, it is a crucial need to enlarge the cavities in hydrophobic interface regions for attracting a lot of attentions of researchers in microemulsion-based studies.

Cage-like molecules/assemblies with three-dimensional(3D) porous cavities of different sizes and shapes are one of the most important supramolecular hosts[19—21]. Currently, a wide variety of cage-like molecules/assemblies with large cavities have been fabricated by using rigid noncoplanar units as the building blocks directly or incorporating noncoplanar units into the building blocks[22]. Tetraphenylethylene(TPE) with four symmetrical highly-twisted phenyl rings has an inherent propeller-like structure and four symmetrical reaction positions[23]. The intrinsic properties of TPE enable it to serve as an excellent building block for fabricating a wide variety of 3D cage-like molecules/assemblies[24—26]. The well-defined cavities in the TPE-based cages have been used for incorporating various guests to achieve gas adsorption and separation, drug encapsulation and release, phase-transfer catalysis, and tunable spectroscopic properties(*e.g.*, optical sensors, imaging labels, and white-emitting devices)[22—26]. Therefore, it is reasonable to anticipate that the incorporation of the propeller-shaped TPE into the double-tailed surfactant backbone could self-assemble into the cage-like hydrophobic interface regions in microemulsions.

In this contribution, the TPE group was covalently linked with two octyl chains(di-C8, nonpolar part) and an anionic sulfonate headgroup through a methoxybutyl spacer(SS, polar

✉ LU Chao
luchao@mail.buct.edu.cn
State Key Laboratory of Chemical Resource Engineering, Beijing University of Chemical Technology, Beijing 100029, P. R. China

https://doi.org/10.1007/s40242-020-0296-7

part), respectively, to fabricate a kind of double-tailed anionic surfactant(we called it as TPE-di-C8SS) with cone-shaped geometry. TPE-di-C8SS could easily form the optically transparent w/o microemulsions in isooctane without the aid of a cosurfactant. Self-assembly of propeller-like TPE near the water-oil interface could induce the formation of 3D cavities between the adjacent TPE-di-C8SS molecules(Fig.1). The presence of large cavities in hydrophobic interface regions, which were named as hydrophobic interface cages(HICs) in water/TPE-di-C8SS/isooctane microemulsion, was addressed by comparing their extraction efficiency towards cationic rhodamine B with water/AOT/isooctane microemulsion. With all other factors(*i.e.*, solvents, headgroups, extraction mechanism, size of water droplets) being equal, the extraction efficiency of rhodamine B using TPE-di-C8SS microemulsion(90%) was nearly twice that of AOT microemulsion(54%). The results revealed that the HICs in microemulsions play a crucial role in the improvement of the extraction efficiency towards rhodamine B. This work not only opens a new way into the development of microemulsions with HICs but also offers a great promise for microemulsion-based applications.

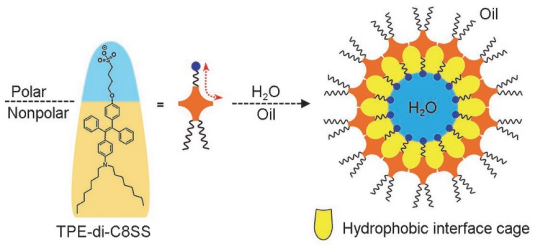

Fig.1 Schematic illustration for hydrophobic interface cages in TPE-di-C8SS microemulsion

Cavities in hydrophobic interface regions were developed through the extra spacer and steric hindrance between rigid TPE groups.

2 Experimental

2.1 Materials

Sodium bis(2-ethylhexyl) sulfosuccinate(AOT), 4-aminobenzophenone, and 4-hydroxybenzophenone were purchased from Tianjin Heowns Biochem LLC(Tianjin, China). Sodium hydride(NaH), 1-bromooctane($C_8H_{17}Br$), and 1,4-butylenesulfone were purchased from Tokyo Chemical Industry(Tokyo, Japan). Rhodamine B was purchased from Fuchen Chemical Reagent Co., Ltd.(Tianjin, China). Anhydrous tetrahydrofuran(THF), ethanol, zinc dust, and titanium tetrachloride($TiCl_4$) were purchased from J&K Chemical Ltd.(Beijing, China). Sodium *tert*-butoxide, anhydrous potassium carbonate(K_2CO_3), and magnesium sulphate($MgSO_4$) were purchased from Energy Chemical(Shanghai, China). Methanol, acetone, petroleum ether(PE), ethyl acetate(EA), dichloromethane(DCM), and isooctane were of analytical reagent grade, and purchased from Beijing Chemical Reagent Company(Beijing, China). Water used in all the experiments was purified with a Milli-Q purification system.

2.2 Synthesis of Intermediate 1

4-Aminobenzophenone(0.98 g, 5.0 mmol) was charged in a 100-mL dry twin-neck flask equipped with a magnetic stirring bar. Anhydrous THF(30 mL) was added under nitrogen atmosphere, and the solution was stirred and cooled to –5 °C. After the addition of NaH(0.6 g, 15 mmol, 60% in oil), the cold bath was removed to make the mixture warm to room temperature. 1-Bromooctane(2.6 g, 15 mmol) was added and reacted with the above mixture for 24 h. The reaction was slowly quenched by ice water drop by drop. The crude product was extracted with DCM, dried over $MgSO_4$, concentrated, and purified by silica gel column chromatography[eluent: *V*(PE)/*V*(EA)=10/1] to give 1.81 g(86%) of a disubstituted product. ^{1}H NMR(400 MHz, $CDCl_3$), δ: 0.87—0.90(t, 6H), 1.25—1.33(m, 20H), 1.60—1.62(m, 4H), 3.31—3.34(t, 4H), 6.60—6.61(m, 2H), 7.42—7.44(m, 2H), 7.49—7.51(m, 1H), 7.71—7.72(m, 2H), 7.76—7.78(m, 2H).

2.3 Synthesis of Intermediate 2

Intermediate **1**(0.84 g, 2.0 mmol), 4-hydroxy-benzophenone (0.40 g, 2.0 mmol), and zinc powder(1.31 g, 20 mmol) were charged in a 100-mL dry twin-neck flask equipped with a magnetic stirring bar. Anhydrous THF(30 mL) was added under nitrogen atmosphere, and the solution was stirred and cooled to –5 °C. $TiCl_4$(1.09 mL, 1.89 g, 10 mmol) was added drop by drop, and the cold bath was removed to make the mixture warm to room temperature. This reaction was carried out in refluxing THF for 10 h, and then quenched by 10% K_2CO_3 aqueous solution. The crude product was extracted with DCM, dried over $MgSO_4$, and purified by silica gel column chromatography[eluent: *V*(PE)/*V*(EA)=10/1] to give 0.38 g(32%) of a yellow solid. ^{1}H NMR(400 MHz, $CDCl_3$), δ: 0.87—0.90(t, 6H), 1.23—1.31(m, 20H), 1.48—1.55(m, 4H), 3.12—3.21(m, 4H), 6.30—6.37(m, 2H), 6.49—6.62(m, 2H), 6.74—6.96(m, 4H), 6.97—7.14(m, 10H).

2.4 Synthesis of TPE-di-C8SS

Intermediate **2**(0.58 g, 1.0 mmol) and sodium *tert*-butoxide(0.38 g, 4.0 mmol) were charged in an 80-mL dry twin-neck flask equipped with a magnetic stirring bar. Anhydrous ethanol(15 mL) was added under nitrogen atmosphere, and the resulted solution was stirred at room temperature for 2 h.

https://doi.org/10.1007/s40242-020-0296-7

1,4-Butylenesulfone(122 μL, 163 mg, 1.2 mmol) was added slowly to the above solution, and reacted with it for 48 h at 80 °C. Without the quenching process, the crude product was directly concentrated and purified by silica gel column chromatography[eluent: *V*(DCM)/*V*(MeOH)=8/1] to give 0.32 g(43%) of a yellow solid. ^{1}H NMR(400 MHz, DMSO-d_6), δ: 0.81—0.89(t, 6H), 1.19—1.27(m, 20H), 1.37—1.47(m, 4H), 1.64—1.76(m, 4H), 2.41—2.48(m, 2H), 3.06—3.21(m, 4H), 3.79—3.89(m, 2H), 6.28—6.39(m, 2H), 6.59—6.73(m, 4H), 6.75—7.17(m, 12H). ^{13}C NMR(400 MHz, DMSO-d_6), δ: 156.87, 156.76, 144.28, 139.84, 139.79, 137.45, 137.42, 131.72, 130.91, 130.87, 130.84, 127.53, 127.48, 113.62, 113.47, 110.43, 110.33, 67.09, 67.05, 51.06, 49.94, 31.17, 28.78, 28.65, 26.79, 26.76, 26.41, 26.37, 22.03, 21.82, 13.90. MS, *m*/*z*: 722.4246([M–Na]$^-$, calculated for $C_{46}H_{60}NO_4S$, 722.4249).

2.5 Preparation of Water-in-oil(w/o) Microemulsions

Two types of w/o microemulsions were prepared as follows: 37.6 mg of TPE-di-C8SS(0.05 mmol) or 23.4 mg of AOT(0.05 mmol) was charged, respectively, in two 20-mL screw-capped vials with magnetic stirring bars. Then, 10 mL of isooctane(as the oil phase) and 18 μL of H_2O were sequentially added and stirred at room temperature until the solutions became optically transparent.

2.6 Sample Characterizations

^{1}H and ^{13}C NMR spectra were carried out using a 400-MHz Bruker spectrometer(Germany). Mass spectrum was collected at room temperature on a Waters Quattro micro-triple quadrupole mass spectrometer(USA). The sizes of microemulsion droplets in different microemulsions were determined by a Malvern Zetasizer 3000HS nano-granularity analyzer(UK). The prepared microemulsion samples were added to the quartz cuvette, and dispersant was set to isooctane[viscosity: 0.5300 cP(1 cP=1 mPa·s), refractive index: 1.391, dielectric constant: 1.94]. The types of water in microemulsion were studied using a Nicolet 6700 Fourier-transform infrared(FTIR) spectrometer(USA). The ultraviolet-visible(UV-Vis) absorption spectra were measured on a Hitachi UV-3900H(Japan). All the characterizations were carried out at room temperature.

3 Results and Discussion

3.1 Design and Synthesis of TPE-di-C8SS

The short-chain cosurfactants at the water-oil interface of four-component w/o microemulsions could diminish the capacity of cavity modification in hydrophobic interface regions. In contrast, a three-component microemulsion without the aid of a cosurfactant is apt to flexibly modify the hydrophobic interface regions. Obviously, sodium bis(2-ethylhexyl) sulfosuccinate(AOT) is one of the most popular surfactants used in three-component microemulsions. However, the small changes in AOT structure could affect the formation of w/o microemulsions[27—29]. As shown in Fig.2(A), it is the only difference in the structures between AOT and sodium bis(1-hexyl) sulfosuccinate(di-C6SS) that the branched double-chain tails on AOT are replaced by the linear double-chain tails on di-C6SS [28]. In comparison with AOT(*ca*. 1.1—1.2 nm), the extended width of di-C6SS decreased to *ca*. 0.8 nm. However, di-C6SS could only form four-component w/o microemulsions using hexanol as a cosurfactant, different from three-component w/o AOT microemulsions[Fig.2(B)]. The steric hindrance between the branched double-chain tails of AOT is indispensable to form three-component w/o microemulsions. By virtue of the molecular width of rigid TPE group(*ca*. 1.1 nm), the incorporation of TPE group into the di-C6SS skeleton could increase the molecular width from *ca*. 0.8 nm to *ca*. 1.1 nm [Fig.2(C)], which would facilitate the formation of three-component w/o microemulsions with 3D HICs. Moreover, the first four carbons adjacent to the ionic headgroup are polar and hydrated by the penetration of water molecules[14—16]. It could be anticipated that a methoxybutyl spacer between sulfonate headgroup and TPE group might further enlarge HICs without affecting the formation of three-component microemulsion.

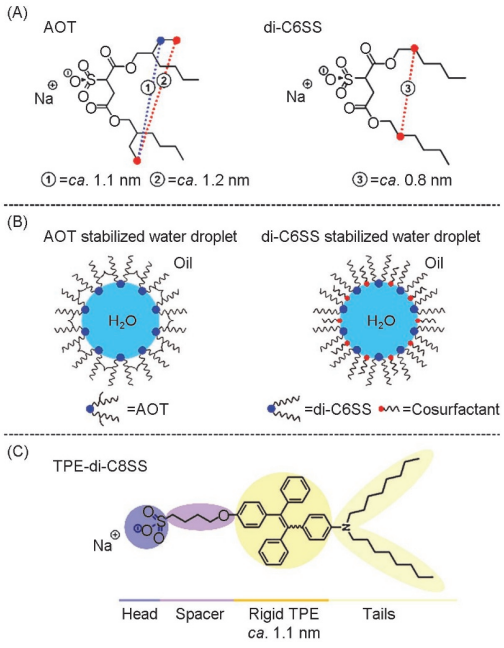

Fig.2 Design of TPE-di-C8SS

(A) Chemical structures of AOT and di-C6SS; (B) illustrations for ternary AOT microemulsion and quaternary di-C6SS microemulsion; (C) chemical structure of TPE-di-C8SS.

https://doi.org/10.1007/s40242-020-0296-7

The synthetic strategy of well-designed TPE-di-C8SS is shown in Fig.3(A). Firstly, two long alkyl chains were introduced into 4-aminobenzophenone: the amine group of 4-aminobenzophenone was fully activated by using an excess of sodium hydride, followed by reacting with an excess of 1-bromooctane to obtain intermediate **1** with di-C8 alkyl chains[30—32]. The propeller-shaped TPE group was introduced through McMurry coupling reaction between 4-hydroxybenzophenone and intermediate **1**[31]. After removal of the coupling by-products of intermediate **1** itself and 4-hydroxybenzophenone itself, intermediate **2** was obtained with di-C8 alkyl chains on one side and a hydroxyl group on the other side. The molecular structures of the intermediates **1** and **2** were characterized and verified by ^{1}H nuclear magnetic resonance(NMR) spectroscopy(Figs.S1 and S2, see the Electronic Supplementary Material of this paper). Finally, intermediate **2** was transformed into a sodium salt in a very alkaline environment and then reacted with 1,4-butanesultone for introducing a sulfonate headgroup to generate TPE-di-C8SS[30—32]. In the ^{1}H NMR spectrum(Fig.S3, see the Electronic Supplementary Material of this paper), the resonance peaks of all hydrogen atoms of intermediate **2** were presented, and three more alkyl hydrogen resonance peaks were appeared due to the introduction of butyl group[Fig.3(B)], indicating the formation of TPE-di-C8SS. The ^{13}C NMR spectrum also verified the structure of TPE-di-C8SS(Fig.S4, see the Electronic Supplementary Material of this paper). Moreover, in the negative-ion mass spectrum(Fig.S5, see the Electronic Supplementary Material of this paper), the mass-to-charge(m/z) ratio of 722.4246 was identified with the molecular weight of TPE-di-C8SS without Na^+, further confirming the synthesis of TPE-di-C8SS[Fig.3(C)].

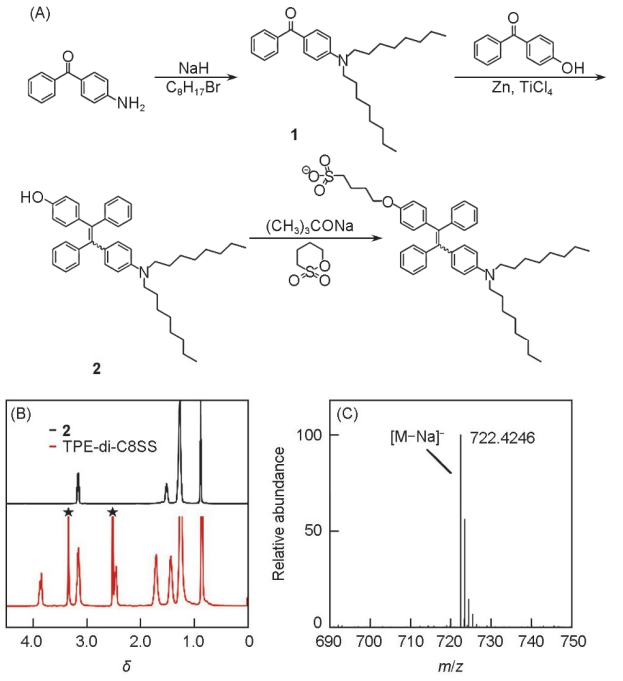

Fig.3 Synthesis and characterization of TPE-di-C8SS

(A) Synthetic strategy for amphiphilic TPE-di-C8SS; (B) comparison of the ^{1}H NMR spectra of intermediate **2** and TPE-di-C8SS in the δ region of 0.0—4.5 (the solvent peaks are marked with asterisks); (C) negative-ion mass spectrum of TPE-di-C8SS.

3.2 Preparation and Characterization of TPE-di-C8SS Microemulsion

According to the ternary water/AOT/isooctane microemulsion system, we examined the ability of the well-designed TPE-di-C8SS to prepare the optically transparent w/o microemulsion without the help of cosurfactant. As shown in Fig.4(A), when water was added to the isooctane solution of TPE-di-C8SS (ω=[H_2O]/[TPE-di-C8SS]=20), the immiscibility between water and isooctane immediately induced poor transparency for the water/TPE-di-C8SS/isooctane mixture solution. After stirring for 4 h, the cloudy mixture solution in a 20-mL screw-capped vial was transformed to be homogeneous and transparent. Moreover, the size distribution of the transparent water/TPE-di-C8SS/isooctane microemulsion was studied by dynamic light scattering(DLS) measurement[Fig.4(B)]. The average diameter of TPE-di-C8SS microemulsion was *ca.* 8.4 nm, indicating the presence of nanometer-sized particles. These results indicated that TPE-di-C8SS has the similar ability with AOT to form three-component w/o microemulsions.

The combined analyses of Fourier transform

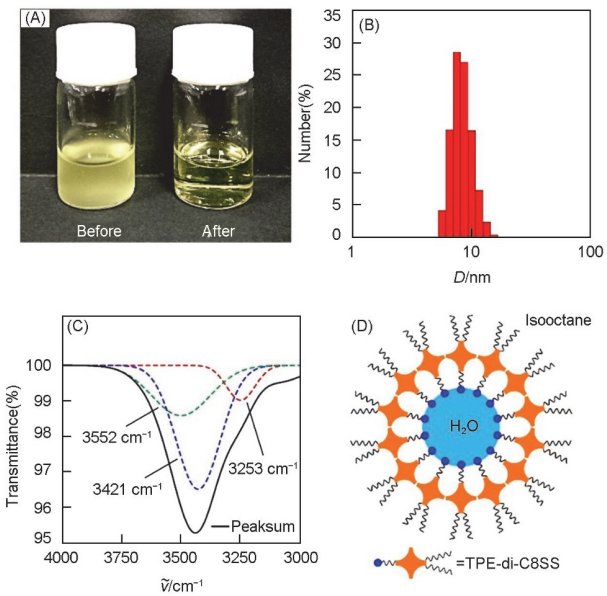

Fig.4 Preparation and characterization of TPE-di-C8SS microemulsion

(A) The photographs of the water/TPE-di-C8SS/isooctane mixture solution before(left) and after(right) stirring for 4 h under a daylight lamp; (B) DLS size distribution; (C) FTIR spectra of the transparent water/TPE-di-C8SS/isooctane mixture solution; (D) schematic diagram for TPE-di-C8SS microemulsion with hydrophobic interface cages.

https://doi.org/10.1007/s40242-020-0296-7

infrared(FTIR) spectroscopy and Gaussian curve fitting were used to identify how many types of water were in the transparent water/TPE-di-C8SS/isooctane mixture solution in order to further confirm the formation of water droplets in TPE-di-C8SS microemulsion[33—36]. Based on the well-characterized AOT microemulsion, there are three types of water in water droplets: (1) trapped water between the surfactant polar groups, (2) bound water at the water-oil interface, and (3) free water in the core[9,33—36]. It is generally recognized that the different O—H stretching vibrations from three types of water in water droplets could lead to different characteristic infrared absorption bands in the range of 3800—3000 cm^{-1}. As shown in Fig.4(C), the infrared absorption bands of the O—H stretch region in the transparent water/TPE-di-C8SS/isooctane mixture solution were measured. The solid line obtained from FTIR spectrometer could serve as a sum of Gaussian peaks, which could be fitted with three independent Gaussian peaks(dotted lines). The low-wavenumber peak centered at around 3253 cm^{-1} was due to the O—H stretch of free water, the 3421 cm^{-1} peak was assigned to the O—H stretch of bound water, and the high-wavenumber peak at 3552 cm^{-1} was resulted from the O—H stretch of trapped water[33—36]. The above investigations demonstrated that the as-prepared TPE-di-C8SS could form the transparent three-component w/o microemulsion with nanometer-sized water droplets.

For AOT w/o microemulsion, the nanometer-sized water droplets were stabilized by a monolayer of AOT molecules at the oil-water interface with their hydrophobic tails towards the oil phase and sulfonate headgroups towards the water phase[9,33—36]. In comparison, TPE-di-C8SS w/o microemulsion was assumed to have the same nanometer-sized water droplets, which were stabilized by a TPE-di-C8SS monolayer[Fig.4(D)]. We concluded that the TPE-di-C8SS sulfonate headgroups at the water-oil interface do not completely shield the water droplets due to their Coulomb repulsion. Moreover, due to the aggregation-induced emission(AIE) feature of TPE, the steric hindrance between the propeller-shaped TPE groups could be demonstrated by detecting the fluorescence of TPE-di-C8SS w/o microemulsion. As shown in Fig.S6(see the Electronic Supplementary Material of this paper), its fluorescence excitation and emission peaks are about 432 and 512 nm, respectively. Thus, the propeller-shaped TPE groups instead of the bulky branched chains could also help to stabilize the surfactant monolayer, facilitating the formation of HICs.

3.3 Evaluation of HICs in TPE-di-C8SS Microemulsion

To verify the role of HICs, two kinds of w/o microemulsions, water/AOT/isooctane microemulsion and water/TPE-di-C8SS/isooctane, were prepared with the same size of water droplets to compare their extraction behaviors under the same conditions. The average radius of water droplets could be obtained by subtracting the molecular length of the surfactant molecule from the average particle radius of the microemulsion[36]. DLS measurements showed that the average particle radii of water/AOT/isooctane microemulsion(Fig.S7, see the Electronic Supplementary Material of this paper) and water/TPE-di-C8SS/isooctane microemulsion[Fig.4(B)] were *ca*. 2.6 and 4.2 nm, respectively. The molecular length of AOT was *ca*. 1.2 nm[36], while the molecular length of TPE-di-C8SS was estimated to be *ca*. 2.8 nm through the calculation from ACD/Labs software. The obtained radii of water droplets in AOT microemulsion and TPE-di-C8SS microemulsion were *ca*. 1.4 nm. When water droplets and headgroups remain the same, it is possible to address whether the differences in the sizes of HICs[Fig.2(B) and 4(D)] determine the extraction efficiencies.

Cationic rhodamine B was selected as the extraction model for the following two reasons: (1) it could be electrostatically attracted to water droplets of negatively charged AOT and TPE-di-C8SS microemulsions, and (2) it was easily tracked by the naked eye owing to its deep pink color[36]. As shown in Fig.5(A), 1.5 mL of 30 μmol/L rhodamine B in aqueous solution was added to two quartz cuvettes, and then 2.5 mL of AOT microemulsion and TPE-di-C8SS microemulsion were added to the above two quartz cuvettes, respectively. With the increase of extraction time, the dark pink color of rhodamine B in aqueous solution gradually became lighter for both AOT and TPE-di-C8SS microemulsions. For AOT microemulsion, the pink color of rhodamine B in aqueous solution almost unchanged over time, indicating that the extraction equilibrium has been reached with moderate extraction efficiency. On the other hand, the color of rhodamine B extracted by TPE-di-C8SS microemulsion continued to fade until it became almost colorless. These photographic observations of rhodamine B in aqueous solution demonstrated that TPE-di-C8SS microemulsion has much better extraction performances than AOT microemulsion with the same size of water droplets.

The changes in the concentrations of rhodamine B were determined by UV-Vis absorption spectroscopy in order to further quantify the extraction efficiency of rhodamine B. Firstly, the extraction of rhodamine B by isooctane was carried out over the range of periods from 1 min to 160 min to exclude the potential effects of isooctane. UV-Vis absorption spectra [Fig.5(B)] indicated that isooctane could not extract rhodamine B in aqueous solution. Then, UV-Vis absorption spectra of aqueous rhodamine B with a series of concentrations(1, 5, 10, 20, and 30 μmol/L) were recorded(Fig.S8, see the Electronic Supplementary Material of this paper). The linear relationship between the absorbance at 550 nm and the rhodamine B

https://doi.org/10.1007/s40242-020-0296-7

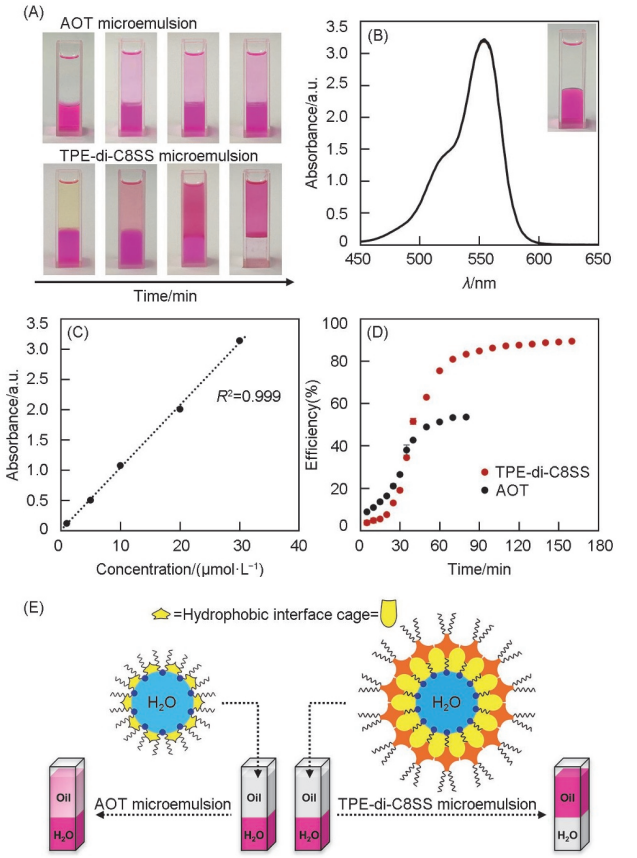

Fig.5 Evaluation of hydrophobic interface cages in TPE-di-C8SS microemulsion

(A) The photographs of the extraction of rhodamine B by AOT microemulsion and TPE-di-C8SS microemulsion at different time(1, 40, 80 and 160 min) under room light; (B) UV-vis absorption spectra of 30 μmol/L rhodamine B in water after extraction by isooctane at different time(1, 40, 80, and 160 min). Inset shows the picture of a mixture of the upper colorless isooctane and the lower pink rhodamine B aqueous solution under room light; (C) linear relationship between the absorbance at 550 nm and the concentration of rhodamine B in water; (D) extraction efficiency(%) of rhodamine B in water after extraction by AOT microemulsion and TPE-di-C8SS microemulsion at different time(min); (E) schematic of hydrophobic interface cages in AOT microemulsion and TPE-di-C8SS microemulsion for the extraction of pink rhodamine B under the same conditions(*i.e.*, temperature, solvents, headgroups, and water droplets).

concentration was established and plotted in Fig.5(C): A=0.1035c+0.0086(R^2=0.999). Extraction efficiency(%) could be calculated according to Equation(1)[37],

$$\text{Efficiency}(\%) = (A_0 - A_t)/A_0 \times 100\% \quad (1)$$

where A_0 represents the absorbance at 550 nm of 30 μmol/L of rhodamine B in aqueous solution, A_t represents the absorbance at 550 nm of the remaining rhodamine B at different time points.

In situ UV-Vis absorption spectra of rhodamine B in aqueous solutions after extraction by AOT microemulsion (Fig.S9, see the Electronic Supplementary Material of this paper) and TPE-di-C8SS microemulsion(Fig.S10, see the Electronic Supplementary Material of this paper) were recorded over the range of periods from 5 min to 160 min to obtain the values of A_t. As shown in Fig.5(D), the calculated extraction efficiencies were plotted as the function of time(min). Obviously, AOT and TPE-di-C8SS microemulsions had a similar trend in extracting rhodamine B in aqueous solution, meaning that both of them have a similar extraction mechanism. On the other hand, AOT microemulsion reached the extraction saturation with an extraction efficiency of 54% at 80 min, while TPE-di-C8SS microemulsion reached the maximum extraction efficiency(90%) at 160 min. Moreover, cationic methylene blue(Fig.S11, see the Electronic Supplementary Material of this paper) was also extracted by the same AOT and TPE-di-C8SS microemulsions. As shown in Figs.S12 and S13(see the Electronic Supplementary Material of this paper), the corresponding extraction efficiency is monitored by UV-Vis absorption spectroscopy. AOT and TPE-di-C8SS microemulsions reached the extraction saturation with an extraction efficiency of 75%(at 40 min) and 86%(at 160 min), respectively. The differences in the extraction efficiencies between AOT microemulsion and TPE-di-C8SS microemulsion clearly demonstrated the crucial role of HICs on microemulsion-based applications.

The driving force for extracting rhodamine B into both TPE-di-C8SS and AOT microemulsions was further examined to ensure that they have the same electrostatically driven extraction mechanism[38]. The addition of NaCl in microemulsions could hinder the electrostatic attraction between cationic rhodamine B and anionic sulfonate because of the effective shielding of the charged surface by salt solution[39]. The water/TPE-di-C8SS/isooctane microemulsion and water/AOT/isooctane microemulsion were prepared in the presence of 1.0 mmol/L NaCl. Their extraction behaviors were monitored by recording the UV-Vis absorption spectra of rhodamine B in aqueous solutions at different time(Figs.S14 and S15, see the Electronic Supplementary Material of this paper). The obtained extraction efficiencies from the changes in absorbance at 550 nm were plotted *versus* time(Fig.S16, see the Electronic Supplementary Material of this paper). It could be found that the extraction efficiencies of rhodamine B in both TPE-di-C8SS[Fig.S16(A)] and AOT microemulsion systems [Fig.S16(B)] in the presence of 1.0 mmol/L NaCl decreased significantly, owing to the weakened Coulomb attraction between anionic sulfonate and cationic rhodamine B. These results further revealed that both TPE-di-C8SS and AOT microemulsions indeed have the same electrostatically driven extraction mechanism. Therefore, the actual role of HICs in TPE-di-C8SS microemulsion[Fig.5(E)] was well addressed by comparing their extraction efficiency towards rhodamine B with AOT microemulsions under the same conditions(*i.e.*, temperature, solvents, headgroups, and water droplets).

4 Conclusions

We have incorporated TPE into two octyl chains and an anionic

https://doi.org/10.1007/s40242-020-0296-7

sulfonate headgroup to synthesize a novel kind of double-tailed anionic TPE-di-C8SS surfactant. The key role of HICs in microemulsions has been addressed by comparing their extraction efficiencies of water-soluble cationic rhodamine B in both AOT and TPE-di-C8SS microemulsion systems with the same size of water droplets and headgroups. The markedly higher extraction efficiency of TPE-di-C8SS microemulsion towards rhodamine B was attributed to the fact that the four highly-twisted phenyl rings in TPE-di-C8SS enable it to form the HICs in microemulsions. Overall, our findings lead to a comprehensive and detailed insight into the important role of HICs in microemulsions. We believe that this strategy may provide an exciting future direction for designing other advanced surfactants with tunable HICs.

Electronic Supplementary Material

Supplementary material is available in the online version of this article at http://dx.doi.org/10.1007/s40242-020-0296-7.

Acknowledgements

This work was supported by the National Natural Science Foundation of China(Nos.21974008, 21804006, 21521005, and 21705035), and the Fundamental Research Funds for the Central Universities, China(No.buctrc201820).

Availability of Data and Materials

All data generated or analyzed during this study are included in this published article and its supplementary information files.

Conflicts of Interest

The authors declare no conflicts of interest.

References

[1] Nowothnick H., Blum J., Schomacker R., *Angew. Chem. Int. Ed.*, **2011**, *50*, 1918
[2] Pera-Titus M., Leclercq L., Clacens J.-M., De Campo F., Nardello-Rataj V., *Angew. Chem. Int. Ed.*, **2015**, *54*, 2006
[3] Luisi P. L., *Angew. Chem. Int. Ed. Engl.*, **1985**, *24*, 439
[4] Chelazzi D., Giorgi R., Baglioni P., *Angew. Chem. Int. Ed.*, **2018**, *57*, 7296
[5] Senske M., Smith A. E., Pielak G. J., *Angew. Chem. Int. Ed.*, **2016**, *55*, 3586
[6] Chapman R., Stenzel M. H., *J. Am. Chem. Soc.*, **2019**, *141*, 2754
[7] Gyger F., Bockstaller P., Gerthsen D., Feldmann C., *Angew. Chem. Int. Ed.*, **2013**, *52*, 12443
[8] Wolf S., Feldmann C., *Angew. Chem. Int. Ed.*, **2016**, *55*, 15728
[9] Levinger N. E., *Science*, **2002**, *298*, 1722
[10] Correa N. M., Silber J. J., Riter R. E., Levinger N. E., *Chem. Rev.*, **2012**, *112*, 4569
[11] Faeder J., Ladanyi B. M., *J. Phys. Chem. B.*, **2000**, *104*, 1033
[12] Abel S., Sterpone F., Bandyopadhyay S., Marchi M., *J. Phys. Chem. B*, **2004**, *108*, 19458
[13] Crans D. C., Levinger N. E., *Acc. Chem. Res.*, **2012**, *45*, 1637
[14] Garcia-Rio L., Leis J. R., Moreira J. A., *J. Am. Chem. Soc.*, **2000**, *122*, 10325
[15] Moilanen D. E., Fenn E. E., Wong D., Fayer M. D., *J. Am. Chem. Soc.*, **2009**, *131*, 8318
[16] Long J. A., Rankin B. M., Ben-Amotz D., *J. Am. Chem. Soc.*, **2015**, *137*, 10809
[17] Sedgwick M., Cole R. L., Rithner C. D., Crans D. C., Levinger N. E., *J. Am. Chem. Soc.*, **2012**, *134*, 11904
[18] Crans D. C., Rithner C. D., Baruah B., Gourley B. L., Levinger N. E., *J. Am. Chem. Soc.*, **2006**, *128*, 4437
[19] Hasell T., Zhang H. F., Cooper, A. I., *Adv. Mater.*, **2012**, *24*, 5732
[20] Garcia-Simon C., Garcia-Borras M., Gomez L., Parella T., Osuna S., Juanhuix J., Imaz I., Maspoch D., Costas M., Ribas X., *Nat. Commun.*, **2014**, *5*, 5557
[21] Cook T. R., Stang P. J., *Chem. Rev.*, **2015**, *115*, 7001
[22] Feng H.-T., Yuan Y.-X., Xiong J.-B., Zheng Y.-S., Tang B. Z., *Chem. Soc. Rev.*, **2018**, *47*, 7452
[23] Mei J., Leung N. L. C., Kwok R. T. K., Lam J. W. Y., Tang B. Z., *Chem. Rev.*, **2015**, *115*, 11718
[24] Zhang C., Wang Z., Tan L., Zhai T.-L., Wang S., Tan B., Zheng Y.-S., Yang X.-L., Xu H.-B., *Angew. Chem. Int. Ed.*, **2015**, *54*, 9244
[25] Zhang M., Saha M. L., Wang M., Zhou Z., Song B., Lu C., Yan X., Li X., Huang F., Yin S., Stang P. J., *J. Am. Chem. Soc.*, **2017**, *139*, 5067
[26] Feng H.-T., Lam J. W. Y., Tang B. Z., *Coord. Chem. Rev.*, **2020**, *406*, 213142
[27] Nave S., Eastoe J., Heenan R. K., Steytler D., Grillo I., *Langmuir*, **2002**, *18*, 1505
[28] Nave S., Eastoe J., Heenan R. K., Steytler D., Grillo I., *Langmuir*, **2000**, *16*, 8741
[29] Nave S., Paul A., Eastoe J., Pitt A. R., Heenan R. K., *Langmuir*, **2005**, *21*, 10021
[30] Guan W., Zhou W., Lu C., Tang B. Z., *Angew. Chem. Int. Ed.*, **2015**, *54*, 15160
[31] Guan W., Wang S., Lu C., Tang B. Z., *Nat. Commun.*, **2016**, *7*, 11811
[32] Guan W., Yang T., Lu C., *Angew. Chem. Int. Ed.*, **2020**, *59*, 12800
[33] Jain T. K., Varshney M., Maitra A., *J. Phys. Chem.*, **1989**, *93*, 7409
[34] Onori G., Santucci A., *J. Phys. Chem.*, **1993**, *97*, 5430
[35] Temsamani M. B., Maeck M., Hassani I. E., Hurwitz H. D., *J. Phys. Chem. B*, **1998**, *102*, 3335
[36] De T. K., Maitra A., *Adv. Colloid Interface Sci.*, **1995**, *59*, 95
[37] Yao Q., Wang S., Shi W., Lu C., Liu G., *Ind. Eng. Chem. Res.*, **2017**, *56*, 583
[38] Rahdar A., Almasi-Kashi M., Khan A. M., Aliahmad M., Salimi A., Guettari M., Kohne H. E. G., *J. Mol. Liq.*, **2018**, *252*, 506
[39] Fathi H., Kelly J. P., Vasquez V. R., Graeve O. A., *Langmuir*, **2012**, *28*, 9267